2024 European Control Conference (ECC)
June 25-28, 2024. Stockholm, Sweden

Concurrent Li-ion Battery Parameter Estimation and Open-Circuit Voltage Reconstruction via L1-Regularized Least Squares

Yang Wang, Riccardo M.G. Ferrari and Michel Verhaegen

***Abstract*— Identification of lithium-ion (Li-ion) battery models is essential for enhancing the operation of electrical vehicles. This paper develops a novel approach for estimating the equivalent circuit model (ECM) of Li-ion batteries and reconstructing the open-circuit voltage (OCV) and state of charge (SOC) relationship. We formulate the OCV-SOC relation as a piecewise affine (PWA) function and estimate its coefficients and the Markov parameters (impulse response) of the ECM via l_1-regularized least squares. The state space model of the ECM is derived through the Ho-Kalman algorithm. Experiments with simulated and real-life battery data demonstrate the method's effectiveness and advantages with respect to the state of the art.**

I. Introduction

Electrical vehicles (EVs) have become indispensable in the quest for sustainable transportation [1] [2]. Lithium-ion (Li-ion) batteries, owing to their high energy density, efficiency, and extended service life, have been widely adopted in EVs [3]. To guarantee application safety and optimize performances, an accurate battery model is fundamental.

Equivalent circuit models (ECMs), owing to an attractive balance between accuracy and computational costs, have been widely used [4]. ECMs emulate electrochemical dynamics by interconnecting elements such as resistors, capacitors, and voltage sources. This approach avoids the use of expensive Partial Differential Equation (PDEs), leading to a low-order system of Ordinary Differential Equations (ODEs).

Identification of the ECM dynamics presents known challenges, such as distinct timescales, parameter dependency on battery aging and working conditions, and the nonlinear relationship between the cell's open-circuit voltage (OCV) and the state of charge (SOC). The OCV-SOC relationship is instrumental in the on-line estimation of the SOC [5]: however, the OCV is not measurable during battery operation.

One solution is to conduct dedicated, static tests to determine a set of OCV-SOC value pairs. The remaining part of the model can then be identified via linear system identification techniques, such as subspace methods [6], [7]. These approaches, however, are time-consuming as they require extended cell resting time [8]. In addition, the OCV-SOC relation depends on temperature and the cell's aging.

To tackle these issues, online OCV estimation was proposed. In [5], [9], for instance, recursive least squares (RLS) are used to track the OCV value during battery operation. These approaches, however, assume the OCV value to be constant across consecutive sampling instants, leading to an oscillatory estimation and being sensitive to measurement noise.

Yang Wang, Riccardo M.G. Ferrari, and Michel Verhaegen are with the Delft Center for Systems and Control, Delft University of Technology, Delft 2628CD, Netherlands. Email: {y.wang-40, r.ferrari, m.verhaegen}@tudelft.nl.

Contributions: In this paper, we develop a novel approach for ECM parameter estimation and OCV-SOC reconstruction using cells' operational data, without the need for dedicated OCV tests. We formulate the OCV-SOC relationship as a piecewise affine (PWA) function. The PWA coefficients, along with the Markov parameters [10] of the ECM linear part, are jointly identified by solving an l_1-regularized least squares problem [11]. With the obtained Markov parameters we derive the state space model of the ECM using the Ho-Kalman algorithm [12]. The effectiveness of the developed method is verified on a simulated battery cell and the fidelity of the OCV estimation is compared to that of existing RLS methods. Our approach is further demonstrated on real-life cell data from simulated EV driving conditions.

The rest of the paper is structured as follows. Section II describes the ECM of Li-ion batteries and the PWA formulation for OCV-SOC reconstruction. Section III presents our parameter estimation approach. Section IV verifies the proposed method on a simulated and on a real NMC/Graphite Li-ion cell. Finally, Section V gives some concluding remarks.

Notations: Throughout this paper, we use the following notations. $A^\dagger$ is the Moor-Penrose pseudo-inverse of A. $\|\cdot\|_F$, $\|\cdot\|_1$, and $\|\cdot\|_2$ are, respectively, the Frobenius norm, l_1 norm, and l_2 norm. Operator $\circ$ is the element-wise product. $\mathrm{diag}(\cdot)$ returns a diagonal matrix. We use $\mathbb{Z}_i^j$ to denote the set $\{i, i+1, \ldots, j\}$, and $x(k:k+l) = [x(k), x(k+1), \ldots, x(k+l)]^\top$ to denote a collection of samples $x(k)$ from time k to $k+l$.

II. Lithium-ion battery model

In this work, we employ the widely used second-order Thevenin model as the ECM for Li-ion batteries, as shown in Figure 1. This model consists of an ideal voltage source v_{oc}, an ohmic resistor R_0, and two resistor-capacitor (RC) circuits. v_{oc} represents the open-circuit voltage (OCV) of the cell and the voltages v_1, v_2 across the two RC circuits

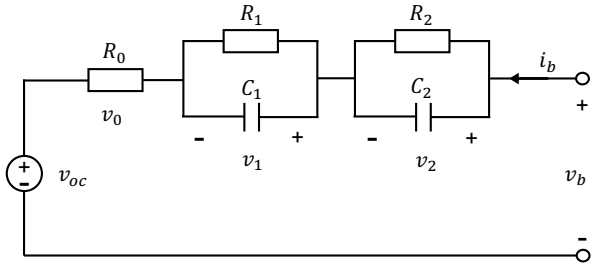

Fig. 1. Second-order Thevenin model

emulate the diffusion voltages caused by the polarization process of the battery. i_b is the load current and v_b is the terminal voltage. The current direction is positive when the cell is being charged. With zero-order hold discretization, we write the ECM dynamics in the following discrete-time state space representation,

$$\begin{aligned} x(k+1) &= Ax(k) + Bu(k) \\ y(k) &= Cx(k) + Du(k) + v_{oc}(k) \end{aligned} \tag{1}$$

where the state $x = \begin{bmatrix} v_1 & v_2 \end{bmatrix}^\top \in \mathbb{R}^2$ is the vector of diffusion voltages; the input $u = i_b$ and the output $y = v_b$ are respectively the load current and the terminal voltage. Matrices $A \in \mathbb{R}^{2\times 2}$ and $B \in \mathbb{R}^2$ are the state and the input matrices of the model,

$$A = \begin{bmatrix} e^{-\frac{T_s}{R_1 C_1}} & 0 \\ 0 & e^{-\frac{T_s}{R_2 C_2}} \end{bmatrix},\ B = \begin{bmatrix} R_1(1 - e^{-\frac{T_s}{R_1 C_1}}) \\ R_2(1 - e^{-\frac{T_s}{R_2 C_2}}) \end{bmatrix},$$

and $C = \begin{bmatrix} 1 & 1 \end{bmatrix} \in \mathbb{R}^2$ and $D = R_0$ are the output matrix and the feed-through term. T_s is the sampling time of the measured data. The OCV is a static nonlinear function of the state of charge (SOC). The SOC describes the amount of charge in a cell relative to its total capacity. It can be computed by integrating the current in discrete time as

$$z(k+1) = z(k) + \frac{\eta T_s}{3600 \times Q} i_b(k) \tag{2}$$

where $z \in [0, 1]$ is the SOC, $\eta \in (0, 1)$ is the charge-discharge efficiency and $Q \in \mathbb{R}^+$ is the total capacity of the battery cell in Ampere-hours (Ah). Multiplication by 3600 converts Ah to Coulombs. Throughout this paper, we make the following assumption about the values of η and Q and the ambient temperature during battery operation:

Assumption 1 *The charge-discharge efficiency η is approximated to one and the total capacity Q equals the nominal capacity. We assume a constant ambient temperature during battery operation throughout this study.*

This assumption is commonly adopted in the literature [13] [14] as the efficiency of Li-ion batteries is typically high (over 98%) [15], and the identification is performed for a fresh cell in a short time of the battery life, which does not cause significant changes in capacity relative to its nominal value. The ambient temperature is kept constant for simplicity and can be achieved using a thermal chamber in which the cell is operated. We furthermore assume that:

Assumption 2 *ECM parameters are constant for the SOC range from 20% to 80%.*

The last assumption is supported by the fact that the parameter variation within this range is negligible [7] [13]. Nevertheless, we will estimate the ECM parameters that best represent the overall behavior of battery cells in the mean square sense within this SOC range.

To reconstruct the OCV-SOC function, we formulate the OCV as a piecewise affine (PWA) function of the SOC as

$$v_{oc} = c_0^j(z) + c_1^j(z) \times z,\ j \in \mathbb{Z}_1^l, \tag{3}$$

where coefficients $c_0^j, c_1^j \in \mathbb{R}$ are piecewise constants that depend on z, and $l \in \mathbb{Z}^+$ is the number of segments that can be designed by the user. This formulation allows for incorporating the prior knowledge that OCV has a functional dependence on the SOC into our identification framework to provide an enhanced OCV estimation.

The battery modeling problem aims to estimate the system matrices (A, B, C, D) of the ECM (1) and the piecewise constant coefficients $c_0^j, c_1^j,\ j \in \mathbb{Z}_1^l$ in (3) using the input-output measurements of the cell. The estimation method is stated in the next section.

III. Battery model identification

The estimation of the system matrices (A, B, C, D) and the PWA function coefficients c_0^j, c_1^j is twofold: first, we identify the Markov parameters [10] of the ECM and the affine function coefficients c_0^j, c_1^j by solving an l_1-regularized least squares problem [11]. Second, the system matrices are retrieved from the identified Markov parameters using the Ho-Kalman algorithm [12] and suitable matrix transformations [16].

A. Estimation of the Markov parameters and OCV function

Based on the state space representation (1), the output at time k can be written as the convolution between the Markov parameters and the past inputs $u(k-p:k)$ as

$$\begin{aligned} y(k) = CA^p x(k-p) + \sum_{i=0}^{p-1} CA^i B u(k-i-1) + \\ Du(k) + v_{oc}(k) \end{aligned} \tag{4}$$

where $p \in Z^+$ is the length of the past time window. Since the battery system is stable, the first term $CA^p x(k-p)$ in (4) converges to zero as the time window p goes to infinity. For a sufficiently large p, we can approximate $y(k)$ by

$$y(k) \simeq \sum_{i=0}^{p-1} CA^i B u(k-i-1) + Du(k) + v_{oc}(k). \tag{5}$$

This formulation decouples the dynamics of the ECM and the OCV value, enabling a separate treatment for each component, yielding a convenient design for OCV estimation.

With the output equation defined in (5), we formulate a data equation covering the future time window as

$$Y_m = U_m G + V_{oc} \tag{6}$$

where $Y_m, V_{oc} \in \mathbb{R}^{m+1}$ are sequences of $y(k)$ and $v_{oc}(k)$,

$$Y_m = \begin{bmatrix} y(k+p) \\ y(k+p+1) \\ \vdots \\ y(k+p+m) \end{bmatrix},\ V_{oc} = \begin{bmatrix} v_{oc}(k+p) \\ v_{oc}(k+p+1) \\ \vdots \\ v_{oc}(k+p+m) \end{bmatrix},$$

$U_m \in \mathbb{R}^{(m+1)\times(p+1)}$ is the Hankel matrix of $u(k)$,

$$U_m = \begin{bmatrix} u(k) & u(k+1) & \cdots & u(k+p) \\ u(k+1) & u(k+2) & \cdots & u(k+p+1) \\ \vdots & \vdots & \ddots & \vdots \\ u(k+m) & u(k+m+1) & \cdots & u(k+p+m) \end{bmatrix},$$

and $G \in \mathbb{R}^{p+1}$ is the vector of Markov parameters,

$$G_{\text{rev}} = \begin{bmatrix} D & CB & CAB & \cdots & CA^{p-1}B \end{bmatrix}^\top, \quad (7)$$

where subscript "rev" denotes reversing the blocks (with D at the end) to align with the notational convention in system identification. The data sequence starts with time $k+p$ such that the responses of unknown inputs and states before time k are negligible. In the data equation (6), both G and V_{oc} are unknown parameters. To estimate them, we formulate the following least squares problem,

$$\min_{G, V_{oc}} \|Y_m - U_m G - V_{oc}\|_F^2. \quad (8)$$

By solving this problem, the Markov parameters G can be directly identified, while the estimation of V_{oc} in this form may overfit the measurement noise and be less accurate.

To provide a more robust estimation, we incorporate the prior knowledge that OCV is functionally dependent on the SOC into V_{oc} using the PWA function (3). Since the PWA function is defined over SOC and the V_{oc} is defined over time, we operate the data sequences such that each SOC point has a unique pair of coefficients regardless of when it appears in time. To do so, we compute a SOC sequence $Z_m \in \mathbb{R}^{m+1}$ with (2) that covers the same interval as Y_m, and then we sort it in descending order into $Z_m^{st} \in \mathbb{R}^m$. Now we define the vectors of the PWA coefficients, $C_{0,m}^{st}(z), C_{1,m}^{st}(z) \in \mathbb{R}^{m+1}$, in (3) for the ordered SOC Z_m^{st} for estimation. This ensures that each pair of coefficients corresponds to a unique SOC point in Z_m^{st} (see Remark 1). By restoring the sequence order, we can convert $C_{0,m}^{st}, C_{1,m}^{st}$ back into the original order of Z_m, aligned with that of the time sequence of V_{oc}. This procedure results in the V_{oc} as

$$V_{oc} = \text{res}\{C_{0,m}^{st}(z)\} + \text{res}\{C_{1,m}^{st}(z)\} \circ Z_m, \quad (9)$$

where $\text{res}\{\cdot\}$ is the restoring operation that converts the vector into the original order of Z_m. This can be achieved by using the sorting index of Z_m^{st}.

Remark 1 *In this formulation, we assume that the values of SOC in Z_m are unique. If there exist repeated SOCs, one can first remove the repetitions and define the coefficient vectors for the unique SOC sequence. Then, replicate those that correspond to the same SOCs in their original positions to retrieve the coefficient vectors of the length of Z_m.*

To enforce the coefficients in $C_{0,m}^{st}, C_{1,m}^{st}$ to be piecewise constant, we employ l_1-regularization to the finite differences of c_0^j, c_1^j to impose that most differences are zeros. Since in this formulation, the PWA coefficients c_0^j, c_1^j for each SOC are considered one unknown parameter, i.e., the OCV-SOC is an $m+1$ pieces affine function, solving for the coefficients can be computationally expensive for large data sequences. To speed up the computation, we reduce the number of free variables by partitioning the OCV-SOC function into a smaller number of segments and then apply the l_1-regularization on the reduced vectors of coefficients. To formulate this, we write $C_{0,m}^{st}$ and $C_{1,m}^{st}$ as

$$C_{0,m}^{st}(z) = \mathcal{P}_q C_{0,l}^{st}(z), \; C_{1,m}^{st}(z) = \mathcal{P}_q C_{1,l}^{st}(z), \quad (10)$$

where $C_{0,l}^{st}(z), C_{1,l}^{st}(z) \in \mathbb{R}^l$, $l \leq m+1$ are the reduced vectors of coefficients, and $\mathcal{P}_q \in \mathbb{R}^{m+1\times l}$ is a block diagonal matrix

$$\mathcal{P}_q = \begin{bmatrix} L & & \\ & \ddots & \\ & & L \end{bmatrix}, \quad (11)$$

where $L = \begin{bmatrix} 1, \ldots, 1 \end{bmatrix}^\top \in \mathbb{R}^q$ is a vector of ones, and $q \in \mathbb{Z}^+$ is the length of each segment[1]. Formulation (10) ensures that the entries in the j-th segment of $C_{0,m}^{st}, C_{1,m}^{st}$ are all equal to the j-th element of $C_{0,l}^{st}, C_{1,l}^{st}$. The length l decides the number of segments for partitioning the OCV-SOC function. A larger number gives a denser approximation to the true function while raising a higher computational cost for estimating the coefficients.

With the V_{oc} formulated in (9)(10), we extend (8) into an l_1-regularized least squares problem as

$$\begin{aligned} \min_{\Theta} & \|Y_m - U_m G - \text{res}\{\mathcal{P}_q C_{0,l}^{st}\} - \text{res}\{\mathcal{P}_q C_{1,l}^{st}\} \circ Z_m\|_F^2 \\ & + \lambda_1 \|\mathcal{D} C_{0,l}^{st}\|_1 + \lambda_2 \|\mathcal{D} C_{1,l}^{st}\|_1 \end{aligned} \quad (12)$$

where $\Theta := \{G, C_{0,l}^{st}, C_{1,l}^{st}\}$ is the variable set (dependency of $C_{0,l}^{st}, C_{1,l}^{st}$ on SOC is omitted for simplicity), $\lambda_1, \lambda_2 \in \mathbb{R}^+$ are weighting factors for regularization and $\mathcal{D} \in \mathbb{R}^{l-1\times l}$ is a finite difference matrix that computes the differences between consecutive elements of the vector

$$\mathcal{D} = \begin{bmatrix} 1 & -1 & & \\ & \ddots & \ddots & \\ & & 1 & -1 \end{bmatrix}. \quad (13)$$

The weighting factors λ_1, λ_2 control the sparsity of vectors $\mathcal{D} C_{0,l}^{st}$ and $\mathcal{D} C_{1,l}^{st}$, i.e., the number of zeros of the elements, and thus the rate of change of the coefficients over SOC. A small regularization factor allows for better tracking of the variation but can lead to weaker enforcement of the piecewise constant property.

B. System matrix realization using the Ho-Kalman algorithm

The Ho-Kalman algorithm is a systematic procedure for deriving a state space realization (A, B, C, D) from Markov parameters [12]. This method is robust to measurement noise and has an analytical solution that helps avoid potential pitfalls of local minima and convergence issues.

Let $\hat{G}$ be the estimated Markov parameters, then we

[1]Ideally, q is the quotient of $(m+1)/l$, and if $m+1$ is not divisible by l, one can put the remainder as an extra length to the last column of $\mathcal{P}_q$.

construct a Hankel matrix $\hat{H} \in \mathbb{R}^{s+1\times h+1}$ of $\hat{G}$ as

$$\hat{H} = \begin{bmatrix} \hat{C}\hat{B} & \hat{C}\hat{A}\hat{B} & \cdots & \hat{C}\hat{A}^h\hat{B} \\ \hat{C}\hat{A}\hat{B} & \hat{C}\hat{A}^2\hat{B} & \cdots & CA^{h+1}B \\ \vdots & \vdots & \ddots & \vdots \\ \hat{C}A^s\hat{B} & \hat{C}\hat{A}^{s+1}\hat{B} & \cdots & \hat{C}\hat{A}^{s+h}\hat{B} \end{bmatrix}. \quad (14)$$

Let $\hat{H}^+$ be the rightmost h block columns of $\hat{C}\hat{A}^i\hat{B}$ in $\hat{H}$, $\hat{H}^-$ be the leftmost h block columns in $\hat{H}$, and $\hat{L}$ be the best rank-n approximation of $\hat{H}^-$ obtained via singular value decomposition (SVD), i.e.,

$$\hat{L} = \hat{U}_1\hat{\Sigma}_1\hat{V}_1^\top, \quad (15)$$

where

$$\hat{H}^- = \begin{bmatrix}\hat{U}_1 & \hat{U}_2\end{bmatrix}\begin{bmatrix}\hat{\Sigma}_1 & 0 \\ 0 & 0\end{bmatrix}\begin{bmatrix}\hat{V}_1 & \hat{V}_2\end{bmatrix}^\top, \quad (16)$$

and $\hat{\Sigma}_1 \in \mathbb{R}^{n\times n}$ is a diagonal matrix containing the n largest singular values of $\hat{H}^-$. Let $\hat{\mathcal{O}}_s$ and $\hat{\mathcal{C}}_h$ be respectively, the s extended observability and h extended controllability matrices,

$$\hat{\mathcal{O}}_s = \begin{bmatrix}\hat{C} & \hat{C}\hat{A} & \cdots & \hat{C}\hat{A}^s\end{bmatrix}^\top, \quad (17)$$

$$\hat{\mathcal{C}}_h = \begin{bmatrix}\hat{B} & \hat{A}\hat{B} & \cdots & \hat{A}^h\hat{B}\end{bmatrix}. \quad (18)$$

Since $\hat{H}$ is the product of $\hat{\mathcal{O}}_s$ and $\hat{\mathcal{C}}_h$ and with $\hat{L}$ being an approximation of $\hat{H}$, we estimate $\hat{\mathcal{O}}_s$ and $\hat{\mathcal{C}}_h$ using (15) as

$$\hat{L} = (\hat{U}_1\hat{\Sigma}_1^{1/2})\hat{\Sigma}_1^{1/2}\hat{V}_1^\top \approx \hat{\mathcal{O}}_s\hat{\mathcal{C}}_h. \quad (19)$$

From the estimated $\hat{\mathcal{O}}_s$, $\hat{\mathcal{C}}_h$, and $\hat{G}$ matrices, we can find a system realization (A, B, C, D) of the ECM (1) as: $\hat{D}$ is the first element of $\hat{G}_{\text{rev}}$; $\hat{C}$ is the first 1×2 block of $\hat{\mathcal{O}}_s$; $\hat{B}$ is the first 2×1 block of $\hat{\mathcal{C}}_h$; and $\hat{A} = \hat{\mathcal{O}}_s^\dagger\hat{H}^+\hat{\mathcal{C}}_h^\dagger$.

C. Matrix transformations for system realization of ECM

The obtained system realization in the previous section is unique up to a similarity transformation [17]. To obtain system matrices having the same structure as the ECM in eq. (1), we perform matrix transformations on the estimated state space realization [16]. First, we conduct an eigenvalue decomposition on $\hat{A}$ as

$$\hat{A} = V\bar{A}V^{-1}, \quad (20)$$

where $\bar{A}$ is a diagonal matrix containing the eigenvalues of $\hat{A}$. Substituting $\hat{A}$ in the estimated state space realization (1) constructed with $(\hat{A}, \hat{B}, \hat{C}, \hat{D})$ with (20), and left multiplying V^{-1}, we have

$$V^{-1}x(k+1) = \bar{A}V^{-1}x(k) + V^{-1}\hat{B}u(k) \quad (21)$$

$$y(k) = (\hat{C}V)V^{-1}x(k) + \hat{D}u(k). \quad (22)$$

By letting $\bar{x} = V^{-1}x(k)$, $\bar{B} = V^{-1}\hat{B}$ and $\bar{C} = \hat{C}V$, we obtain a state space model that yields the same input-output behaviors,

$$\bar{x}(k+1) = \bar{A}\bar{x}(k) + \bar{B}u(k) \quad (23)$$

$$y(k) = \bar{C}\bar{x}(k) + \hat{D}u(k). \quad (24)$$

Then, we apply a matrix transformation with $W = \text{diag}(\bar{C})$ to the previous model such that $\tilde{x} = W\bar{x}$, $\tilde{A} = W\bar{A}W^{-1}$, $\tilde{B} = W\bar{B}$, $\tilde{C} = \bar{C}W^{-1}$. W is invertible as the ECM is observable and the identified model preserves the observability, and thus we have $\bar{C} = \hat{C}V \neq 0$. Now we obtain an equivalent state space model in the input-output behaviors as

$$\tilde{x}(k+1) = \tilde{A}\tilde{x}(k) + \tilde{B}u(k) \quad (25)$$

$$y(k) = \tilde{C}\tilde{x}(k) + \hat{D}u(k). \quad (26)$$

In this model realization, we have $\tilde{C} = [1,\ 1]$, and $\tilde{A}$ is a diagonal matrix, which aligns with the structure of the state space model of the ECM (1). This allows us to retrieve the physical parameters. In the next section, we demonstrate the effectiveness of the developed method for ECM identification and OCV-SOC reconstruction in simulation experiments and with real-life cell data.

IV. Numerical experiments with simulated and real-life battery data

To illustrate the effectiveness of the developed method for ECM identification, we apply it first to a simulated cell and then to real-life data. The dataset used in this simulation is from the CALCE dataset [18].

A. Experiment on a simulated model

We constructed a simulated cell with the following electrical elements which represent an NMC/Graphite Li-ion cell as reported in [19],

$$R_0 = 0.07\ \Omega,\quad R_1 = 0.02\ \Omega,\quad R_2 = 0.01\ \Omega,$$
$$C_1 = 500\ F,\quad C_2 = 10000\ F. \quad (27)$$

These elements correspond to a state space representation of the ECM (1) as

$$A = \begin{bmatrix}0.9048 & 0 \\ 0 & 0.9900\end{bmatrix},\quad B = \begin{bmatrix}0.0019 \\ 9.9502\text{e}-05\end{bmatrix}$$
$$C = \begin{bmatrix}1 & 1\end{bmatrix},\quad D = 0.07.$$

To demonstrate the effectiveness of the PWA function for the OCV-SOC reconstruction, we simulated a piecewise affine OCV-SOC function (3) with the following coefficients,

$$c_0 \in \{3.14, 3.24, 3.22, 3.47, 3.52, 3.47, 3.38, 3.26\}$$
$$c_1 \in \{0.99, 0.86, 0.89, 0.39, 0.27, 0.44, 0.88, 2.04\}.$$

These coefficients are obtained from the incremental OCV test, which measures the OCV-SOC value pairs, for a Li-ion cell recorded in the CALCE dataset by connecting the value pairs with a piecewise affine function. The input to the simulated model is the Dynamic Stress Test (DST), which emulates real-life loading conditions of batteries [18], and the output of the simulation is added with white noise with a standard deviation of $5\text{e}-4$. The simulated input is shown in Figure 2.

In this simulation, the l_1-regularized least squares problem (8) was solved in Matlab using the `CVX` [20] toolbox with the Mosek [21] solver, commonly used for large-scale optimization problems. We set the number of piecewise segments (10)

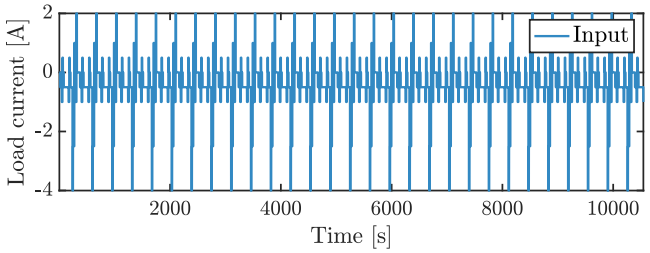

Fig. 2. Dynamic Stress Test Profile

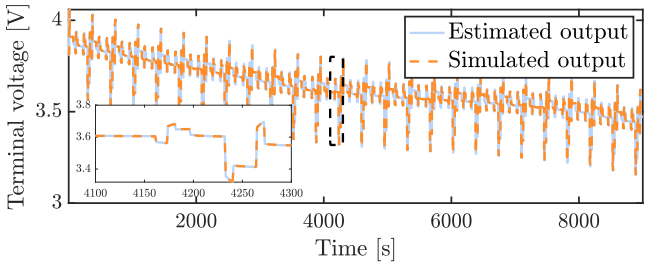

Fig. 3. Output fitting to the simulated data

$l = 20$, and let $\lambda_1 = 5\text{e}-4$, $\lambda_2 = 1\text{e}-4$, and $p = 300$. The sampling time T_s is 1 second according to the measurements in the CALCE dataset. We evaluated the performance of the estimation with the Root Mean Square Error (RMSE) and the Variance-Accounted-For (VAF) metrics defined as

$$\text{RMSE} := \frac{\|y(k) - \hat{y}(k)\|_2}{\sqrt{N}}$$

$$\text{VAF} := (1 - \frac{\frac{1}{N}\sum_{k=1}^{N}\|y(k) - \hat{y}(k)\|_2^2}{\frac{1}{N}\sum_{k=1}^{N}\|y(k)\|_2^2}),$$

where $N \in \mathbb{R}^+$ is the data length. VAF has a value between 0% and 100%; A higher VAF indicates a better fit to the measured data [10].

The performance of the output fitting is shown in Figure 3. The RMSE [V] of the fitting is $5.84\text{e}-04$ and the VAF is 99.99%, indicating a sufficient estimation. Figure 4 shows the estimated Markov parameters on a logarithmic scale. We show the first 30 elements as the later terms are near zero and sensitive to estimation errors. These errors, however, have limited influences on the identified dominant dynamics.

From the identified Markov parameters, we derived the ECM system matrices using the Ho-Kalman algorithm (Section III-B) and matrix transformations (Section III-C) as

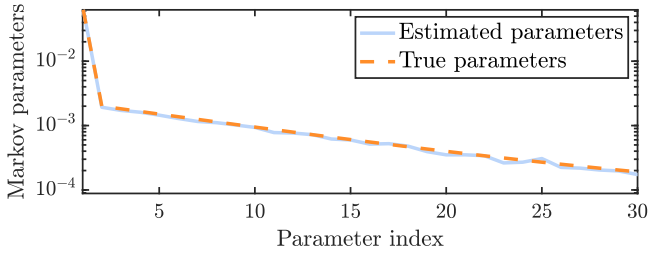

Fig. 4. Markov parameter estimation

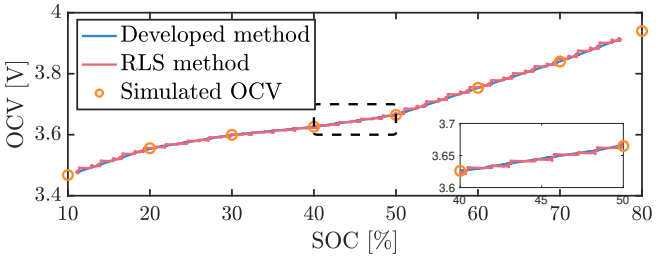

Fig. 5. OCV estimations of the developed and the RLS methods

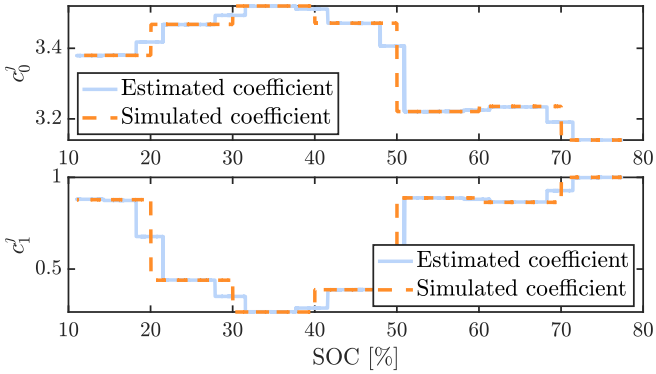

Fig. 6. Estimation of coefficients of piecewise affine OCV function

$$\tilde{A} = \begin{bmatrix} 0.9026 & 0 \\ 0 & 0.9882 \end{bmatrix}, \quad \tilde{B} = \begin{bmatrix} 0.0018 \\ 1.3841\text{e}-04 \end{bmatrix}$$
$$\tilde{C} = \begin{bmatrix} 1 & 1 \end{bmatrix}, \quad \tilde{D} = 0.071.$$

These estimations are consistent with the true parameters with only minor errors.

In the following, we illustrate the effectiveness of the OCV-SOC reconstruction and compare it to the conventional RLS method [5] [9]. The forgetting factor of the RLS method was 0.97. This value was selected in favor of the algorithm to have a balanced performance between tracking speed and oscillation.

Figure 5 shows the reconstructed OCV-SOC function for both the developed and the RLS methods. We see that the developed method generates a smoother and more robust estimation compared to that of the RLS method.

To examine more closely the effectiveness of the PWA formulation for the OCV-SOC function, we show in Figure 6 the PWA coefficients, which present a good alignment with that of the ground-truth parameters.

From this simulation experiment, we verified that the developed identification method can effectively estimate the second-order ECM parameters and reconstruct a smoother OCV-SOC function.

B. Experiment with real-life battery data

In this section, we apply the developed method to real-life battery data. The battery measurements are from the CALCE dataset collected on a LiNiMnCo(NMC)/Graphite Li-ion cell with an 80% initial SOC under the FUDS test at 25°C. The

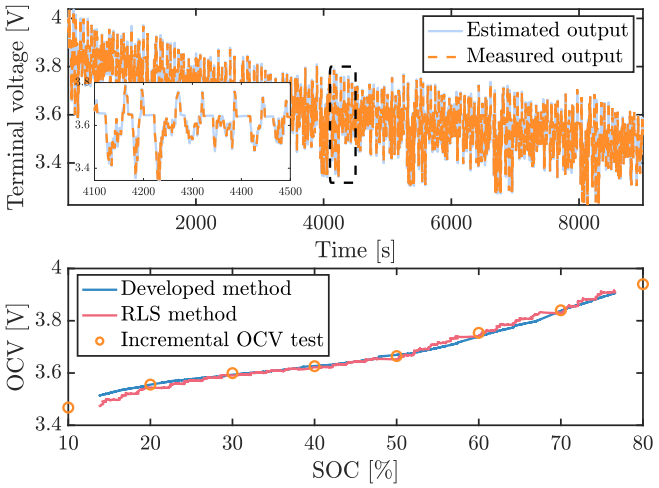

Fig. 7. Output fitting to the measured data and the OCV estimation during the FUDS test at 25 °C

number of OCV-SOC segments was selected as $l = 20$, and the regularization weighting factors were $\lambda_1 = 2\text{e}-6, \lambda_2 = 1\text{e}-6$. We evaluated the model performance based on the output fitting and the OCV-SOC reconstruction due to the lack of ground-truth battery parameters. Figure 7 presents the estimated output and the reconstructed OCV-SOC function of the identified model. The RMSE [V] of the estimated voltage is 0.0016 and the VAF is 100%. The estimated OCV-SOC function is compared with the RLS method and measured OCV-SOC value pairs obtained from the incremental OCV test in the CALCE dataset. This comparison shows that the developed method presents an improved estimation than the existing RLS method and is consistent with the tested cell.

The estimated ECM parameters of the battery cell under test are

$$\tilde{A} = \begin{bmatrix} 0.9616 & 0 \\ 0 & 0.7013 \end{bmatrix}, \quad \tilde{B} = \begin{bmatrix} 0.001 \\ 4.1148\text{e}-04 \end{bmatrix}$$
$$\tilde{C} = \begin{bmatrix} 1 & 1 \end{bmatrix}, \qquad \tilde{D} = 0.0711.$$

The estimation results demonstrate that the identified cell model is effective in predicting the cell's output voltage and reconstructing a smooth and adequately accurate OCV-SOC function, which is the most crucial component for SOC estimation required by a battery cell model used on EVs.

V. Conclusions

In this work, we developed a novel approach for ECM parameter estimation and OCV-SOC reconstruction for Li-ion cells. The OCV-SOC relation was formulated as a piecewise affine function and estimated simultaneously with the Markov parameters of the ECM by solving an l_1-regularized least squares problem. The state space model of the ECM was retrieved from the identified Markov parameters using the Ho-Kalman algorithm with suitable matrix transformations. We showed in simulation experiments that the developed method can effectively estimate the ECM parameters and provide a smoother OCV-SOC reconstruction compared to the conventional RLS method. The developed method was employed on real-life battery data to derive a cell model. Future work will consider temperature and SOC-dependent ECM parameters.

References

[1] I. Husain, B. Ozpineci, M. S. Islam, E. Gurpinar, G.-J. Su, W. Yu, S. Chowdhury, L. Xue, D. Rahman, and R. Sahu, "Electric drive technology trends, challenges, and opportunities for future electric vehicles," *Procs. of the IEEE*, vol. 109, no. 6, pp. 1039–1059, 2021.

[2] J. Meng, G. Luo, M. Ricco, M. Swierczynski, D.-I. Stroe, and R. Teodorescu, "Overview of lithium-ion battery modeling methods for state-of-charge estimation in electrical vehicles," *Applied sciences*, vol. 8, no. 5, p. 659, 2018.

[3] G. L. Plett, *Battery management systems, Volume I: Battery modeling*, vol. 1. Artech House, 2015.

[4] R. Xiong, J. Cao, Q. Yu, H. He, and F. Sun, "Critical review on the battery state of charge estimation methods for electric vehicles," *Ieee Access*, vol. 6, pp. 1832–1843, 2017.

[5] X. Chen, H. Lei, R. Xiong, W. Shen, and R. Yang, "A novel approach to reconstruct open circuit voltage for state of charge estimation of lithium ion batteries in electric vehicles," *Applied Energy*, vol. 255, p. 113758, 2019.

[6] Y. Li, C. Liao, L. Wang, L. Wang, and D. Xu, "Subspace-based modeling and parameter identification of lithium-ion batteries," *Int. J. of Energy Research*, vol. 38, no. 8, pp. 1024–1038, 2014.

[7] B. Xia, X. Zhao, R. De Callafon, H. Garnier, T. Nguyen, and C. Mi, "Accurate lithium-ion battery parameter estimation with continuous-time system identification methods," *Applied energy*, vol. 179, pp. 426–436, 2016.

[8] Y. Xing, W. He, M. Pecht, and K. L. Tsui, "State of charge estimation of lithium-ion batteries using the open-circuit voltage at various ambient temperatures," *Applied Energy*, vol. 113, pp. 106–115, 2014.

[9] J. Tian, X. Liu, S. Li, Z. Wei, X. Zhang, G. Xiao, and P. Wang, "Lithium-ion battery health estimation with real-world data for electric vehicles," *Energy*, vol. 270, p. 126855, 2023.

[10] M. Verhaegen and V. Verdult, *Filtering and system identification: a least squares approach*. Cambridge university press, 2007.

[11] R. Mustata, M. Verhaegen, H. Ohlsson, and F. Gustafsson, "Receding horizon estimation of arbitrarily changing unknown inputs," *IFAC Procs. Volumes*, vol. 47, no. 3, pp. 5939–5944, 2014.

[12] S. Oymak and N. Ozay, "Revisiting ho–kalman-based system identification: Robustness and finite-sample analysis," *IEEE Trans. on Automatic Control*, vol. 67, no. 4, pp. 1914–1928, 2021.

[13] K. Fan, Y. Wan, and B. Jiang, "State-of-charge dependent equivalent circuit model identification for batteries using sparse gaussian process regression," *J. of Process Control*, vol. 112, pp. 1–11, 2022.

[14] C. Zhang, W. Allafi, Q. Dinh, P. Ascencio, and J. Marco, "Online estimation of battery equivalent circuit model parameters and state of charge using decoupled least squares technique," *Energy*, vol. 142, pp. 678–688, 2018.

[15] J. Xiao, Q. Li, Y. Bi, M. Cai, B. Dunn, T. Glossmann, J. Liu, T. Osaka, R. Sugiura, B. Wu, *et al.*, "Understanding and applying coulombic efficiency in lithium metal batteries," *Nature energy*, vol. 5, no. 8, pp. 561–568, 2020.

[16] Y. Hu and S. Yurkovich, "Linear parameter varying battery model identification using subspace methods," *J. of Power Sources*, vol. 196, no. 5, pp. 2913–2923, 2011.

[17] C. Yu, L. Ljung, A. Wills, and M. Verhaegen, "Constrained subspace method for the identification of structured state-space models (cosmos)," *IEEE Trans. on Automatic Control*, vol. 65, no. 10, pp. 4201–4214, 2019.

[18] F. Zheng, Y. Xing, J. Jiang, B. Sun, J. Kim, and M. Pecht, "Influence of different open circuit voltage tests on state of charge online estimation for lithium-ion batteries," *Applied energy*, vol. 183, pp. 513–525, 2016.

[19] Z. Yang and X. Wang, "An improved parameter identification method considering multi-timescale characteristics of lithium-ion batteries," *J. of Energy Storage*, vol. 59, p. 106462, 2023.

[20] M. Grant and S. Boyd, "Cvx: Matlab software for disciplined convex programming, version 2.1," 2014.

[21] M. ApS, *The MOSEK optimization toolbox for MATLAB manual. Version 10.0.*, 2022.